Electronic structure of ZrS_xSe_{2-x} by Tran-Blaha modified Becke-Johnson density functional

A. Ghafari,[1,*] A. Boochani,[2] C. Janowitz,[1] and R. Manzke[1]

[1]*Institut für Physik, Humboldt-Universität zu Berlin, Newtonstraße 15, D-12489 Berlin, Germany*

[2]*Physics Department, Islamic Azad University, Kermanshah Branch, Iran*

(Received 7 April 2011; published 8 September 2011)

The electronic properties of the layered transition metal dichalcogenide ZrS_xSe_{2-x} semiconductors for $x = 0$ and 2 as well as for the ternary compound with $x = 1$ have been calculated by density functional theory for six different exchange-correlation energy approximations by the WIEN2k code. The results show that, among the functions we tested, a new semilocal potential that combines the modified Becke–Johnson potential and the local spin density approximation correlation potential as proposed by Tran and Blaha [F. Tran and P. Blaha, Phys. Rev. Lett. **102**, 226401 (2009)] (TB-MBJ) remains superior for estimating the band gap. Thus, the calculations have been performed within the TB-MBJ method both with and without spin-orbit interaction. Calculations by all methods reveal that the valence band maximum and conduction band minimum are located at the Γ and *M* points, respectively, which are in agreement with experimental data. Moreover, in the three compounds the band gap decreases linearly from ZrS_2 to $ZrSe_2$. When considering spin-orbit (SO) coupling, the degeneracy of the valance bands is removed. The size of the SO splitting increases by the atomic number of chalcogenide from ZrS_2 to $ZrSe_2$.

DOI: 10.1103/PhysRevB.84.125205 PACS number(s): 78.40.Fy, 71.15.Mb

I. INTRODUCTION

The layered 1T-metal dichalcogenides have been found to possess interesting anisotropic optical, mechanical, and transport properties. Observation of charge density waves, superconductivity, sometimes their coexistence in some members, and many technology applications (such as solar cells and fuel cells), cause them to be a unique subject for intensive experimental and theoretical research.[1] Zirconium dichalcogenide compounds have attracted much interest due to their suitability for a number of applications. For instance, recently electrical transport properties and prototype optoelectronic devices based on individual ZrS_2 nanobelts have been discussed in Ref. 2. Moreover, the size of the band gaps of the ternary ZrS_xSe_{2-x} semiconductor series was found to vary almost linearly with the composition parameter x.[3] These materials are discussed as promising candidates for third-generation photovoltaic applications.[3]

The general formula of the dichalcogenides is MX_2 (M the metal and X the chalcogenide) where in this paper M represents Zr and X is Se or S, i.e. the zirconium planes are sandwiched between two sulphur-selenium layers. Therewith, the structure consists of X-M-X atomic trilayer units, which are joined by strong covalent bonds inside the layers, whilst relatively weak van der Waals forces hold the sheets together. ZrS_2 and $ZrSe_2$ have the $P\text{-}3m1$ space group while ZrSeS has the $P3m1$ space group.

There is not any theoretical report for the electronic structure of the ternary compound ZrSeS, although recently experimental measurements of band gaps by optical absorption was discussed by Moustafa *et al.*[3] The authors reported indirect band gaps in the range 1.18–1.7 eV and direct band gaps in the range 1.61–2.10 eV. On the other hand, there are varieties of experimental and theoretical reports of the electronic structure for the two end members, i.e. ZrS_2 and $ZrSe_2$. For instance, Wilson and Yoffe[4] have discussed the electronic properties of ZrS_2 and $ZrSe_2$ from the experimental side.

First calculated band structures of ZrS_2 and $ZrSe_2$ have been reported by Murray *et al.*,[5,6] obtained by the semi-empirical tight binding (TB) linear combination of atomic orbitals (LCAO) method. It revealed that the materials are semiconductors with band gaps of 1.78 and 1.37 eV, respectively. However, there are many different TB variants, ranging from completely semi-empirical to first-principles-based versions.[7] In Ref. 8, the relationship between the semi-empirical TB method with the first-principles method has been discussed comprehensively. The calculation of Bullett[9] based on the chemical pseudopotential revealed different band gaps for ZrS_2 and $ZrSe_2$, which are 1.7 eV and 1.0 eV, respectively. However, the pseudopotential method ignores the dynamics of the core electrons (freezes them) and replaces their effects by an effective potential.[10] Other methods like self-consistent symmetrized orthogonalized plane wave revealed band gaps of about 1.6 and 1.3 eV for ZrS_2 and $ZrSe_2$, respectively.[11,12] All the band structure calculations for the two end members have shown that the valence band maximum (VBM) and the conduction band minimum (CBM) are located at the Γ and *M* points of the Brillouin zone, respectively, but all of them are generally less accurate than methods based on density functional theory (DFT),[13] that is a computationally efficient and often more accurate approach to electronic structure calculation in condensed-matter physics and quantum chemistry. In DFT theory, a self-consistent solution of a one-electron Schrödinger equation is used for the evaluation of the ground-state electron density and total energy E so that the exchange-correlation energy as a functional of the density needs to be approximated in practice. There is only one calculation for ZrS_2 and $ZrSe_2$ by the WIEN97 code[14] of Reshak and Auluck,[15] which is based on the DFT method. The results show that the band gaps are 1.4 and 0.85 eV, respectively.[15] However, the authors did not consider spin-orbit interaction and accurate exchange-correlation energy (which is possible today). The DFT calculation also revealed that these materials are semiconductors and have similar positions for CBM and

VBM when compared to band structures obtained by other theoretical methods.

In this paper, we report results of the electronic structure of ZrS_2 and $ZrSe_2$ as well as the ternary compound ZrSeS by the full-potential linearized augmented plane wave method due to Singh,[16] which is implemented in the package WIEN2K code.[17] Within several different exchange-correlation energy functionals, such as the local spin density approximation (LDA) and the generalized gradient approximation (GGA), one usually underestimates the band gap, but the Engel–Vosko (EV) approximation[18,19] and a new semilocal potential that combines the modified Becke–Johnson potential[20] and the LDA correlation potential (TB-MBJ) as recently proposed by Tran and Blaha[21] deliver theoretical band gaps comparable in size to the experimental results. All hitherto published band structure calculations, however, show that the VBM and the CBM are located at the Γ and M points, respectively, for $ZrSe_2$, ZrS_2 and also due to our calculations for ZrSeS. In addition, our calculation shows how the degeneracy of the top of most valence bands is removed, when we consider spin-orbit coupling in the calculation for the three compounds. As expected the size of the SO splitting increases with the atomic number of the chalcogenide, i.e. from ZrS_2 to $ZrSe_2$.

II. METHOD

The full-potential method is used in the WIEN2k code within the framework of DFT so that the energy is described by

$$E_{\text{tot}} = T_s + V_{ec} + V_{en} + V_{nn} + E_{xc}, \tag{1}$$

where T_s is the kinetic energy of a system of noninteracting electrons, and the three next terms represent the electron-electron electrostatic Coulomb energy, the electron-nucleus electrostatic Coulomb energy, and the nucleus-nucleus electrostatic Coulomb energy, respectively. The last term is the exchange-correlation energy which can be decomposed into its exchange and correlation parts ($E_{xc} = E_x + E_c$). In Eq. (1), only the last part as a functional of the electron spin densities $n\downarrow(r)$ and $n\uparrow(r)$ must be approximated.[22] However, the exact mathematical form of the exchange energy E_x is known, but it is a functional which depends explicitly on the orbital wave function (ψ_i) and leads to calculations which are relatively extensive.[23] On the other hand, for the correlation part E_c no exact form exists which can be used for practical calculations.

There are several approximations for E_{xc} and the WIEN2K code is flexible to use some of them, for instance, Perdew–Burke–Ernzerhof (PBE 96),[22] LDA, Wu-Cohen 2006 (WC),[24] and Perdew *et al.* 2008 (PBEsol).[25] WC, PBE 96, and PBEsol are of GGA form. However, there are two classes of GGA functionals. One are the empirical functionals,[26] whose parameters are determined by fitting experimental or *ab initio* data. The other class are the parameter-free functionals, whose parameters are determined in order to satisfy mathematical relations, which are known to hold for the exact functional.[22,27] LDA and GGA have been reviewed in Refs. 23 and 28.

The exchange-correlation energy in the LDA has the following form:

$$E_{xc}[\rho] = \int \varepsilon_{xc}[\rho(r)]\, d^3r,$$

where ε_{xc} is the exchange-correlation energy per unit volume, which is a function of the electron density [$\varepsilon_{xc} = -\frac{3}{4}(\frac{3}{\pi})^{1/3}\rho^{4/3}$], but in the GGA formalism, instead the gradient of the electron density is used for a better description of atom and molecules. In GGA the exchange-correlation energy is

$$E_{xc}[\rho] = \int \varepsilon_{xc}^{\text{GGA}}[\rho(r), \nabla\rho(r)] d^3r = \int \varepsilon_{xc}^{\text{LDA}}[r_s(r)] F_{xc}[r_s(r), s(r)] d^3r,$$

where F_{xc}, r_s, and s are the enhancement factor, Wigner–Seitz radius, and reduced density gradient, respectively. They can be written in the following form

$$F_{xc}(r_s, s) = F_x(s) + F_c(r_s, s), \quad r_s = \left(\frac{3}{4\pi\rho}\right)^{1/3},$$

$$s = \frac{\nabla\rho}{[2(3\pi^2)^{1/3}\rho^{4/3}]},$$

where the enhancement factor in the PBE and WC are as follows

$$F_x^{\text{PBE}}(s) = 1 + \kappa - \frac{\kappa}{1 + \frac{\mu}{\kappa}s^2},$$

$$F_x^{\text{WC}}(s) = 1 + \kappa - \frac{\kappa}{1 + \frac{x(s)}{\kappa}},$$

where $\kappa = 0.804$, $\mu = 0.21951$, and $x(s) = \frac{10}{81}s^2 + (\mu - \frac{10}{81})s^2 e^{-s^2} + Ln(1 + cs^4)(c = 0.0079325)$.

In the PBEsol functional is$\mu = \frac{10}{81}$,[23] the rest is the same as in PBE.

On the other hand, the TB-MBJ potential has the following form[21]

$$v_{x,\sigma}^{\text{MBJ}}(r) = c v_{x,\sigma}^{\text{BJ}}(r) + (3c - 2)\frac{1}{\pi}\left[\frac{10 t_\sigma(r)}{12\rho_\sigma(r)}\right]^{1/2},$$

where ρ_σ is the electron density, t_σ is the kinetic energy density, $v_{x,\sigma}^{\text{BJ}}$ is the Becke–Roussel potential,[29] which can be written as

$$v_{x,\sigma}^{\text{BJ}}(r) = -\frac{1}{b_\sigma(r)}\left[1 - \frac{1}{e^{x_\sigma(r)}} - \frac{x_\sigma(r)}{2e^{x_\sigma(r)}}\right],$$

and

$$c = \alpha + \beta\left[\frac{1}{V}\int_{\text{cell}} \frac{|\nabla\rho(r\prime)|}{\rho(r\prime)} d^3r\prime\right]^{1/2},$$

where V is the unit volume cell and α, β are two free parameters.

It has been argued that both LDA and GGA approximations usually underestimate the band gaps. Wu and Cohen[24] have shown that their WC functional is a significant improvement over LDA and PBE96 for the geometrical parameters and the bulk modulus of solids. It is believed that PBE is the best approach for solids with 3d transition elements.[23] On the other hand, LDA is still among the best for some classes of solids, e.g. the 5d transition metals.[23] In Refs. 30 and 31, some new GGA approximations have been discussed.

Experimental lattice parameters were used[32] and −8.5 Ry for the energy that separates valence from core states. Subsequently, the k points, $G_{\max}$ and $R_{MT}K_{\max}$ (where R_{MT}

TABLE I. Calculated optimized lattice parameters within the PBEsol functional for $ZrSe_2$, ZrS_2, and ZrSeS with hexagonal crystal structure. The experimental lattice parameters are given in parentheses.

Compound	a, b (Å)	c (Å)	Space group
$ZrSe_2$	3.789 (3.758)[a]	6.165 (6.114)[a]	*P*-3*m*1
ZrS_2	3.654 (3.660)[a]	5.795 (5.804)[a]	*P*-3*m*1
ZrSeS	3.713 (3.709)[a]	6.010 (6.004)[a]	*P*3*m*1

[a]Experimental values from Ref. 32.

represents the smallest muffin-tin radius and $K_{\max}$ is the maximum size of reciprocal lattice vectors) are optimized by starting from $G_{\max} = 12\ (\text{au})^{-1}$, $R_{MT}K_{\max} = 6$ and k points = 100, while the valence wave functions inside the spheres are expanded up to $L_{\max} = 10$. A self-consistent iteration process was repeated until the charge convergence of 0.0000001 e was reached. The self-consistency is obtained using the $G_{\max} = 14\ (\text{au})^{-1}$, 500 k-points mesh in the irreducible Brillouin zone, and $R_{MT}K_{\max} = 8.5$. Using optimized values of $R_{MT}K_{\max}$, $G_{\max}$, and k points and experimental lattice parameters, the volume was optimized by minimizing the total energy of the crystal to the volume in the PBEsol functional, and then the theoretical lattice constants were extracted (Table I). The density of states (DOS) and band structure were calculated for the six different exchange-correlation energies, i.e. PBE 96, LDA, WC, PBEsol, EV, and TB-MBJ by theoretical lattice constants. Additionally, in the case of TB-MBJ, the calculations have been performed with and without spin-orbit interaction.

III. RESULTS AND DISCUSSION

It is a well-known problem with self-consistent band structure calculations within DFT that both LDA and GGA approximations usually underestimate the band gap.[33] Typically, in the DFT calculation the underestimation of the band gap when compared with experimental data is about 30–100%.[34] This could be due to the exchange-correlation energy, which LDA and GGA cannot determine exactly, but it is believed that EV is able to better calculate some properties which mainly depend on the accuracy of exchange-correlation energy, such as band gap. In addition, Tran and Blaha[21] recently proposed a new semilocal potential that combines the modified Becke–Johnson potential[20] and LDA, which gives a similar precision as obtainable with the more expensive hybrid functionals and GW methods, while the TB-MBJ potential is computationally as cheap as LDA or GGA. Therewith, it can obtain accurate band gaps.

After analyzing the results, we have classified them in two groups; the first group contains PBE 96, LDA, WC, and PBEsol and gives similar electronic structures for each compound (i.e. $ZrSe_2$, ZrS_2, and ZrSeS). For each compound, the band gap that is calculated by LDA is distinctly smaller than that from the three other methods EV, TB-MBJ (WSO), and TB-MBJ (SO). The band gaps which are calculated within this first group for $ZrSe_2$, ZrS_2, and ZrSeS are all also significantly less than the experimental values, while there is only one experimental result[3] and no other theoretical calculation for ZrSeS. However, PBEsol derived by Perdew *et al.* contains no empirical parameters, an assertion which has been confirmed for solids by several studies.[31,35] The indirect and direct band gaps calculated by the first group of methods are given in Table II and III, respectively.

The second group contains EV and TB-MBJ as E_{xc} functionals and gives band gaps almost comparable with the experimental results, but obviously EV is not as good as TB-MBJ. Thus, we will discuss the DOS and the band structure which are calculated within TB-MBJ in two modifications: by considering spin-orbit (SO) interaction and without it (WSO). The spin orbit interaction is due to coupling between orbital magnetic moments and spin moments. The Hamiltonian of spin-orbit interaction for an isolated atom is given by

$$H_{\text{SO}} = \frac{1}{2m_e^2c^2r}\frac{\partial V}{\partial r}\mathbf{L}.\mathbf{S},$$

where V is the potential energy of the electron, and L and S are angular momentum and spin momentum, respectively.[36] The interaction of **L.S** is proportional to Ze^2 for a Coulomb potential where Z is the atomic number. Therefore, it grows with Z. Due to spin orbit coupling, the p states are splitting into two states with energy $E_j = E_1 + \lambda_1$ and $E_j = E_1 - 2\lambda_1$ for $j = 3/2$ and $j = 1/2$, respectively (where the λ_1 is a constant). In the case of ZrS_xSe_{2-x}, the valence bands are made mainly of p states (see blow). Therefore, not only the degeneracy of bands is removed by spin-orbit interaction, but also it is expected that the SO splitting increases by the atomic number of the chalcogenide from ZrS_2 to $ZrSe_2$. In the WIEN2K code, this SO interaction can be considered via a second variational method, as discussed in details in Ref. 37.

The results show that among the functions we tested, TB-MBJ remains superior for the estimating of the band gap, such that recently, there are several research papers that have published the evaluation of the electronic structure of solids by the TB-MBJ method.[38,39] It should be mentioned here that we

TABLE II. Comparison of the indirect band gap for $ZrSe_2$, ZrS_2, and ZrSeS where calculated within the six different exchange-correlation energy methods. For the TB-MBJ method the band gap is given by considering with (SO) and without (WSO) spin-orbit interaction. The band gap linearly decreases from ZrS_2 to $ZrSe_2$ in all exchange-correlation energy methods. The energy units are electron volt.

						TB-MBJ		
Compound	PBE 96	LDA	WC	PBEsol	EV	WSO	SO	Experiment (Ref. 3)
ZrS_2	0.967	0.929	0.974	0.968	1.34	1.41	1.40	1.7
ZrSeS	0.78	0.54	0.582	0.72	1.17	1.18	1.13	1.40
$ZrSe_2$	0.56	0.49	0.51	0.51	0.86	0.92	0.81	1.18

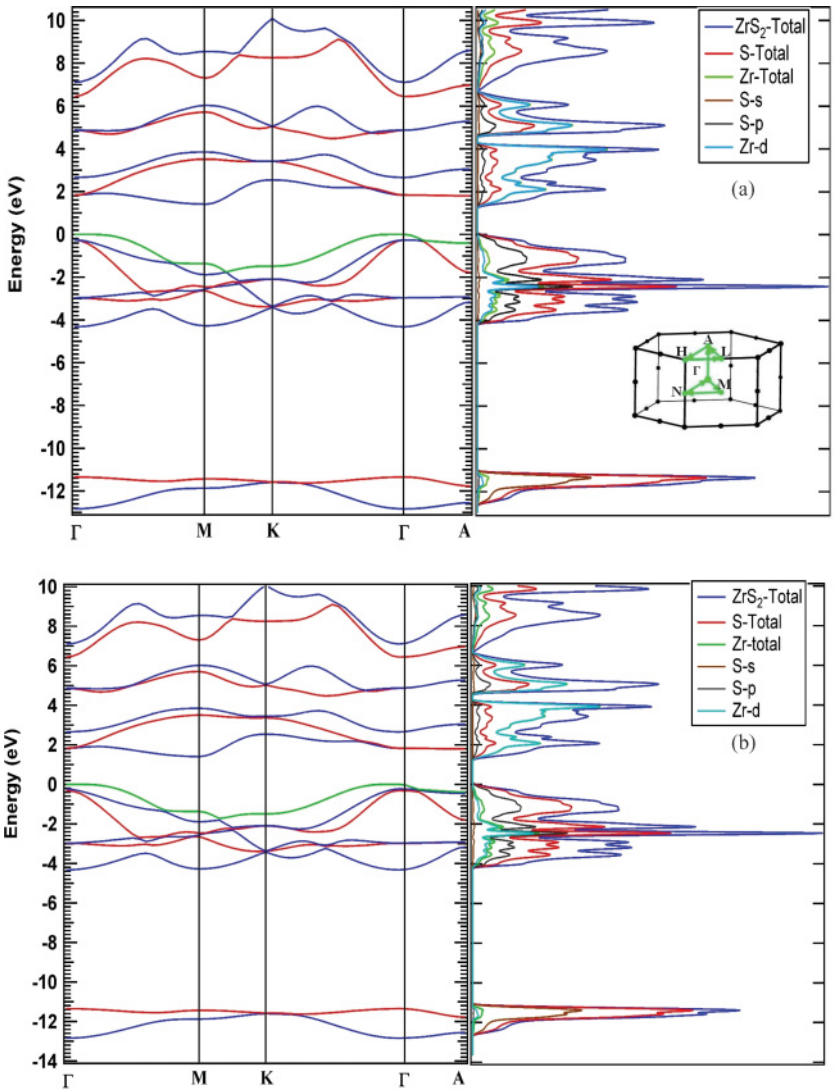

FIG. 1. (Color online) Band structure and DOS of ZrS_2 within the TB-MBJ method by considering (a) without and (b) with spin-orbit interaction in the calculation, where the band gaps are 1.41 and 1.40 eV, respectively. The valence band maximum and conduction band minimum are located at Γ and *M* points, respectively. The SO splitting of the top valence band at the Γ point is about 0.087eV (see b). The inset shows the Brillouin zone.

have chosen the semiconductor compounds, ZrS_xSe_{2-x}, for the present comparison between theory and experiment due to the fact that the topmost valence band is derived dominantly from chalcogen *p* states and that the lowest conduction band is dominantly of Zr *d* character, see also below. Therefore, optical transitions via the band gap are allowed within dipole approximation. This is, hence, the quite rare case where a direct comparison between experimental and theoretical band gaps can be applied.

All the band structure calculations have shown that the VBM and the CBM are located at the Γ and *M* points, respectively, for $ZrSe_2$, ZrS_2, and ZrSeS. For instance for ZrS_2, from Figs. 1(a) and 1(b) we can see that the VBM and CBM are located at the Γ and *M* points, respectively, for both WSO and SO methods. The indirect band gaps are 1.41 and 1.40 eV, respectively. Comparing these values with other methods in Table II, it is clear that TB-MBJ improved the band gap value. However, the band gap decreases when considering SO interaction.

Looking more closely at Fig. 1, four groups of bands can be visually identified. First, the lowest band at −12 eV binding energy has mainly sulphur-*s* state contribution, the second group is from about −4 eV to the Fermi level, which is composed of sulphur-*p* state contribution (in which the

TABLE III. Comparison of the direct band gap for $ZrSe_2$, ZrS_2, and ZrSeS where calculated within the six different exchange-correlation energy methods. For the TB-MBJ method, the direct band gap is given by considering with (SO) and without (WSO) spin-orbit interaction. The band gap linearly decreases from ZrS_2 to $ZrSe_2$ in all exchange-correlation energy methods. The energy units are electron volt.

						TB-MBJ		
Compound	PBE 96	LDA	WC	PBEsol	EV	WSO	SO	Experiment (Ref. 3)
ZrS_2	1.62	1.52	1.57	1.57	1.88	2.05	2.01	2.10
ZrSeS	1.33	1.24	1.28	1.28	1.54	1.66	1.60	1.80
$ZrSe_2$	1.04	0.97	1.01	1.01	1.24	1.35	1.24	1.61

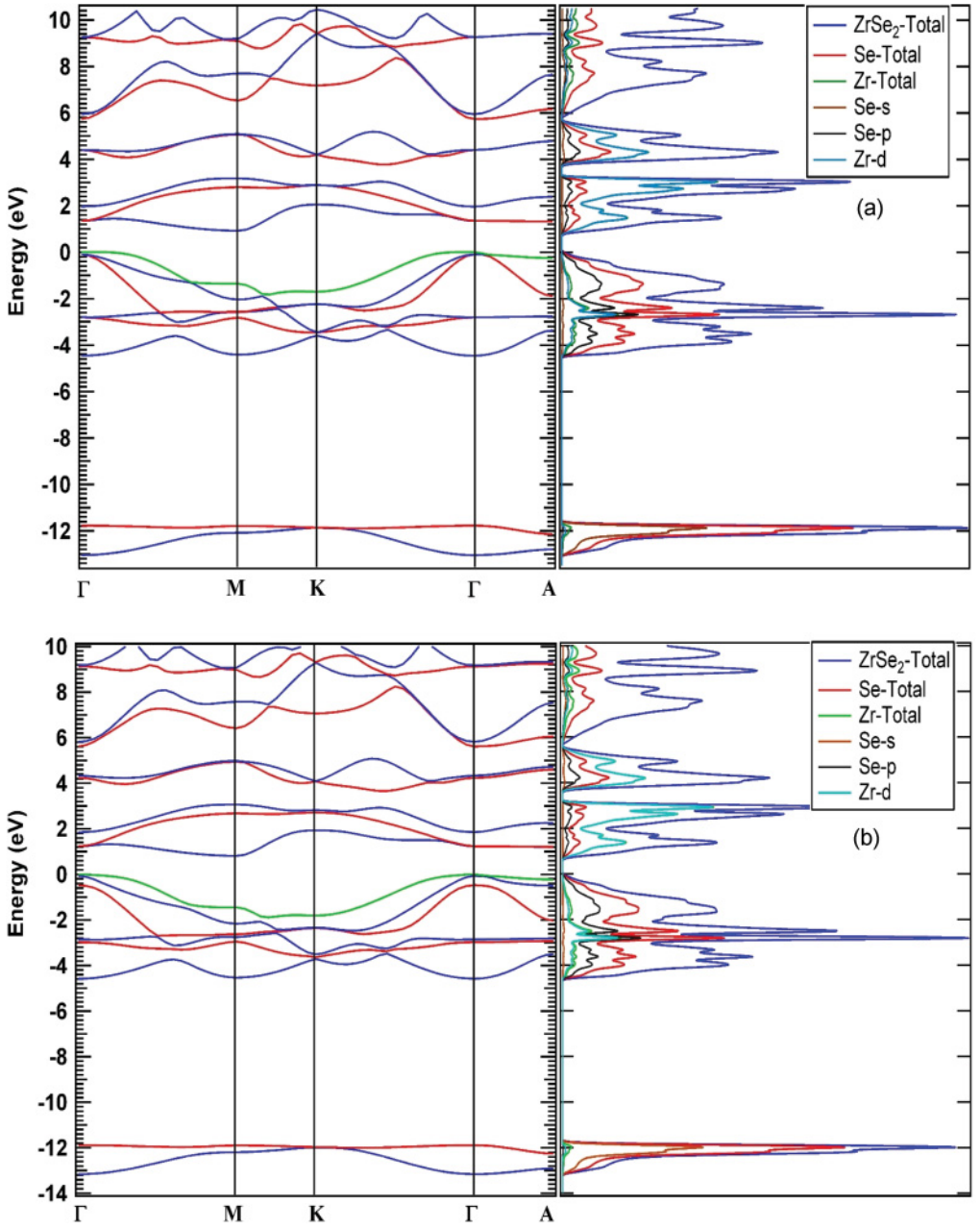

FIG. 2. (Color online) Band structure and DOS of $ZrSe_2$ within the TB-MBJ method by considering (a) without and (b) with spin-orbit interaction in the calculation, where the band gaps are 0.92 and 0.81 eV, respectively. The valence band maximum and conduction band minimum are located at Γ and *M* points, respectively. The splitting of the top valence band at the Γ point is 0.472 eV (see b).

contribution of $p_x + p_y$ is more than p_z) and only a very small contribution from Zr-*d* states (in which the contribution of $d_{xz} + d_{yz}$ is more than the other *d* states). Figure 1(b) reveals how the degeneracy of the valence bands is removed by considering SO interaction. For instance, at the central point of the Brillouin zone, Γ, it is about 0.087 eV for ZrS_2. It cannot be resolved graphically in Fig. 1(a). The third group between 1 and 3 eV is mainly derived from Zr-*d* states and only a very small contribution from sulphur-*p* states, and the last group higher than +5 eV has contributions of Zr-*d* states more than sulphur-*p*.

The band structure and total DOS of $ZrSe_2$ are shown in Fig. 2. It shows similar appearance as ZrS_2 with some minor differences which are: (i) in both methods, the band gap of $ZrSe_2$ is less than ZrS_2, i.e. 0.92 and 0.81 eV for WSO and SO, respectively, while the experimental value is about 1.18 eV.[3] So similar with ZrS_2, the band gap decreases by considering spin-orbit interaction. (ii) The contribution of *p* states at the second group of bands in the case of $ZrSe_2$ is less than ZrS_2. Similar behavior is seen at the total-Se and total-S states density, not only at the second group of bands, but also at the third group. However, the contribution of total-Zr states in both cases is almost the same. (iii) Similarly, as for ZrS_2 described above, the degeneracy of valence bands is removed by SO interaction at the Γ point. For $ZrSe_2$, it is about 0.472 eV. As expected, this is more than the value for ZrS_2 [see Fig. 2(b)].

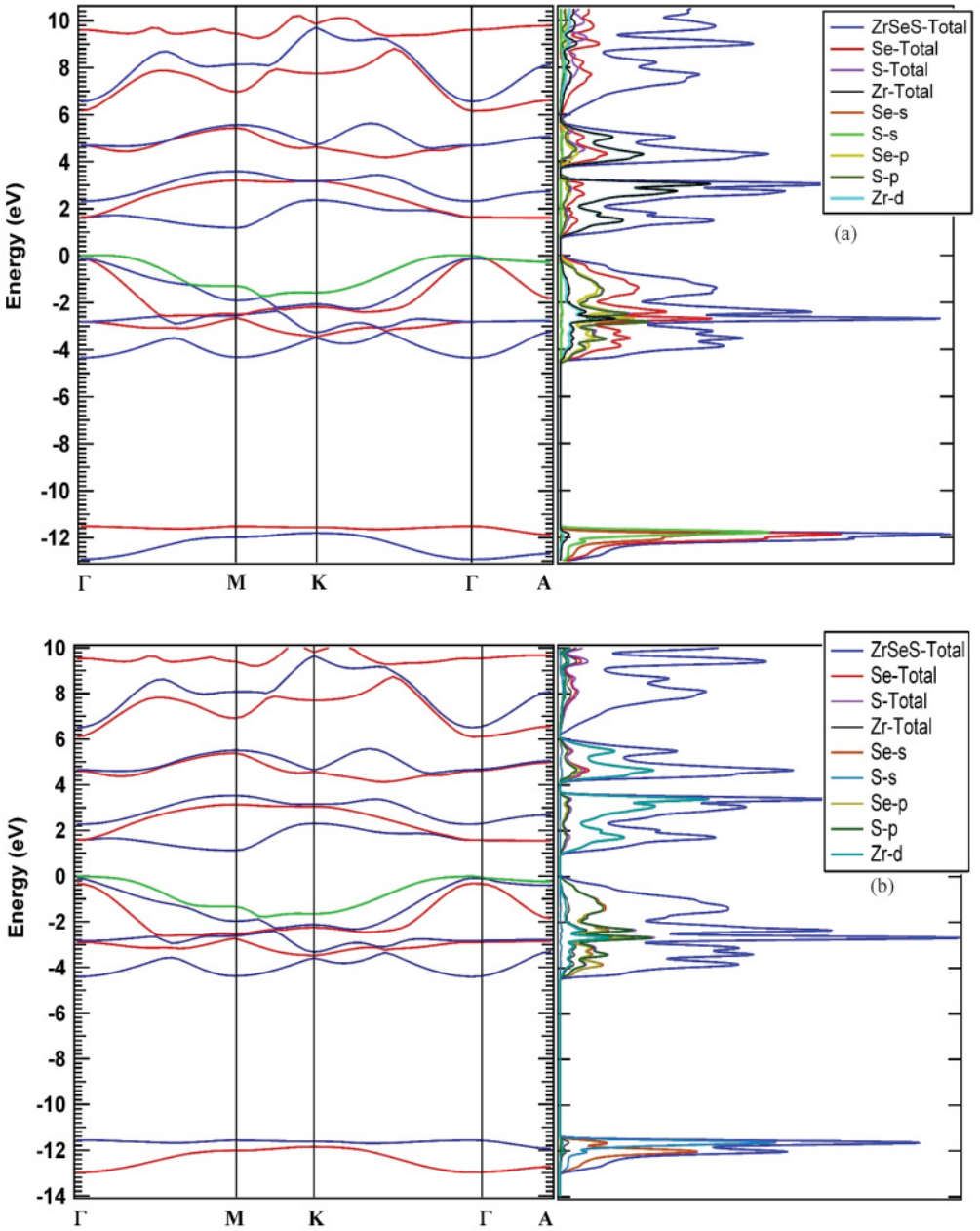

FIG. 3. (Color online) Band structure and DOS of ZrSeS within the TB-MBJ method by considering (a) without and (b) with spin-orbit interaction in the calculation, where the band gaps are 1.18 and 1.13 eV, respectively. The valence band maximum and conduction band minimum are located at Γ and *M* points, respectively. The splitting of the top valence band at the Γ point is 0.236 eV (see b).

For the ternary compound ZrSeS, calculated here for the first time, the total DOS and band structure are depicted in Fig. 3, where the band gap is 1.18 and 1.13 eV for WSO and SO, respectively. An experimental value of about 1.40 eV is reported in Ref. 3. Some significant results on the electronic structure of ZrSeS are: (i) the contribution of S and Se at the lowest band at about 12 eV is almost the same. (ii) The contribution of S-*p* derived states at the second group of bands is a little higher than from Se-*p* derived states, but at the third group of bands from +1 to +6 eV, the S-*p* and Se-*p* contributions are almost the same. (iii) The Zr-*d* states at the third group of bands in ZrSeS and $ZrSe_2$ are the same, but they are a little less in the ZrS_2. Finally, the maximum splitting of the top valence band observed at the Γ point is about 0.236 eV, which is between the values of $ZrSe_2$ and ZrS_2.

There is a strong hybridization in the three compounds between *p* states of S/Se and *d* states of Zr in which the $p_x + p_y$ contribution in the S/Se is higher than that of p_z and also the contribution of $d_{xz} + d_{yz}$ is higher than that of the other Zr-*d* states. This strong in-plane hybridization makes strong covalent bonds inside the layers and weak van der Waals forces between the sheets. In addition, in the three compounds, the band gap linearly decreases from ZrS_2 to $ZrSe_2$.

Tran and Blaha[21] have used the TB-MBJ potential for several solids, such as strongly correlated 3*d* transition metal oxides (e.g. NiO), wide band gap insulators, and small band gap *sp* semiconductors so that they have demonstrated that, for

most cases, the TB-MBJ potential yields band gaps which are in good agreement with experiment, leading to typical errors of less than 10%. Recently, the TB-MBJ potential has also been used for the II-VI-semiconductors CdTe and HgTe by Feng *et al.*,[40] where their results point out that the TB-MBJ potential reveals even for these compounds good agreement with experimental data, while a significant difference is seen in LDA. Therefore TB-MBJ potential has been found as an accurate method for the electronic structure of solids.[38,39,41] Recently, Chan and Ceder[42] have proposed a very new formalism called Δ-sol. We did not apply this formalism here because the authors believed that, for their method, the highest accuracies are obtained for compounds with only *s* and *p* valence electrons.

IV. CONCLUSIONS

In summary, the band structure and DOS of ZrS_2, $ZrSe_2$, and ZrSeS have been calculated by using six different exchange-correlation energy functionals. We were able to classify the results in two groups; the first group contains the methods PBE 96, LDA, WC, and PBEsol, where we do not find significant differences between them in each compound, and the calculated band gaps came out distinctly smaller than in the experiment. The second group contains the methods EV and TB-MBJ, where the band gaps are comparable with experimental results. Finally, the results of the TB-MBJ method extended to spin-orbit interactions have been discussed. Moreover, in the three compounds, the band gap decreases linearly from ZrS_2 to $ZrSe_2$. Similarly, spin-orbit coupling removed the degeneracy of the top valance bands. The size and absolute values of the SO splitting with increasing atomic number of the chalcogenide from ZrS_2 to $ZrSe_2$ is given.

ACKNOWLEDGMENTS

The authors gratefully thank H. Sadat Nabi for discussions. A. Ghafari gratefully thanks for the Yousef Jameel Scholarship.

*aa.ghafari@gmail.com

[1] J. A. Wilson, F. J. Di Salvo, and S. Mahajan, Adv. Phys. **24**, 117 (1975).
[2] L. Li, X. S. Fang, T. Y. Zhai, M. Y. Liao, U. K. Guatam, X. C. Wu, Y. Koide, Y. Bando, and D. Golberg, Adv. Mater. **22**, 4151 (2010).
[3] M. Moustafa, T. Zandt, C. Janowitz, and R. Manzke, Phys. Rev. B **80**, 035206 (2009).
[4] J. A. Wilson and A. D. Yoffe, Adv. Phys. **18**, 193 (1969).
[5] R. B. Murray, R. A. Bromley, and A. D. Yoffe, J. Phys. C **5**, 759 (1972).
[6] R. B. Murray and A. D. Yoffe, J. Phys. C **5**, 3038 (1972).
[7] A. K. McMahan and J. E. Klepeis, Phys. Rev. B **56**, 12250 (1997).
[8] E. Doni, L. Resca, R. Resta, and R. Girlanda, Solid State Commun. **34**, 461 (1980).
[9] D. W. Bullett, J. Phys. C **11**, 4501 (1978).
[10] J. C. Phillips and L. Kleinman, Phys. Rev. **116**, 287 (1959).
[11] P. Krusius, H. Isomaki, and J. von Boehm, J. Phys. C **12**, 3253 (1979).
[12] H. M. Isomaki, J. von Boehm, and P. Krusius, J. Phys. C **12**, 3239 (1979).
[13] W. Kohn and L. J. Sham, Phys. Rev. **140**, A1133 (1965).
[14] P. Blaha, K. Schwarz, and J. Luitz, computer code WIEN97 (Vienna University of Technology, Vienna, 1997) (improved and updated Unix version of the original copyright wien code) which was published by P. Blaha, K. Schwartz, P. Sorantin, and S. B. Trickey, Comput. Phys. Commun. **59**, 399 (1990).
[15] A. H. Reshak and S. Auluck, Physica B **353**, 230 (2004).
[16] D. J. Singh and L. Nordstrom, *Planewaves Pseudopotentials and the LAPW Method*, 2nd ed. (Springer, Berlin, 2006), p. 43.
[17] P. Blaha, K. Schwarz, G. Madsen, D. Kvaniscka, and J. Luitz, *Wien2k, An Augmented Plane Wave Plus Local Orbitals Program for Calculating Crystal Properties* (Vienna University of Technology, Vienna, Austria, 2001).
[18] E. Engel and S. H. Vosko, Phys. Rev. A **47**, 2800 (1993); **47**, 13164 (1993).
[19] Lars Lykke, Bo B. Iversen, and Georg K. H. Madsen, Phys. Rev. B **73**, 195121 (2006); David J. Singh, *ibid.* **81**, 195217 (2010); Briki, A. Zaoui, F. Boutaiba, and M. Ferhat, Appl. Phys. Lett. **91**, 182105 (2007).
[20] A. D. Becke and E. R. Johnson, J. Chem. Phys. **124**, 221101 (2006).
[21] F. Tran and P. Blaha, Phys. Rev. Lett. **102**, 226401 (2009).
[22] J. P. Perdew, K. Burke, and M. Ernzerhof, Phys. Rev. Lett. **77**, 3865 (1996).
[23] P. Haas, F. Tran, P. Blaha, K. Schwarz, and R. Laskowski, Phys. Rev. B **80**, 195109 (2009).
[24] Z. Wu and R. E. Cohen, Phys. Rev. B **73**, 235116 (2006).
[25] J. P. Perdew, A. Ruzsinszky, G. I. Csonka, O. A. Vydrov, G. E. Scuseria, V. N. Staroverov, and J. Tao, Phys. Rev. A **76**, 040501(R) (2007).
[26] E. H. Lieb and S. Oxford, Int. J. Quantum Chem. **19**, 427 (1981).
[27] J. P. Perdew, K. Burke, and M. Ernzerhof, Phys. Rev. Lett. **78**, 1396 (1997).
[28] A. P. Gaiduk and V. N. Staroverov, Phys. Rev. A **83**, 012509 (2011).
[29] A. D. Becke and M. R. Roussel, Phys. Rev. A **39**, 3761 (1989).
[30] P. Haas, F. Tran, and P. Blaha, Phys. Rev. B **79**, 085104 (2009); **79**, 209902(E) (2009).
[31] G. I. Csonka, J. P. Perdew, A. Ruzsinszky, P. H. T. Philipsen, S. Lebègue, J. Paier, O. A. Vydrov, and J. G. Ángyán, Phys. Rev. B **79**, 155107 (2009).
[32] S. G. Patel, S. K. Arora, and M. K. Agarwal, Bull. Mater. Sci. **21**, 297 (1998).
[33] P. Dufek, P. Blaha, and K. Schwarz, Phys. Rev. B **50**, 7279 (1994).
[34] C. S. Wang and W. E. Pickett, Phys. Rev. Lett. **51**, 597 (1983).
[35] Y. Zhao and D. G. Truhlar, J. Chem. Phys. **128**, 184109 (2008).
[36] W. A. Harrison, *Applied Quantum Mechanics* (World Scientific, Singapore, 2000) p. 301.
[37] A. H. MacDonald, W. E. Pickett, and D. D. Koelling, J. Phys. C **13**, 2675 (1980); Lecture note of Pavel Novak (1997) on spin-orbit coupling available from: [http://www.wien2k.at/reg_user/textbooks/novak_lecture_on_spinorbit.ps].
[38] S. Pittalis, E. Räsänen, and C. R. Proetto, Phys. Rev. B **81**, 115108 (2010).
[39] D. J. Singh, Phys. Rev. B **82**, 205102 (2010).
[40] W. Feng, D. Xiao, Y. Zhang, and Y. Yao, Phys. Rev. B **82**, 235121 (2010).
[41] S. Pittalis, E. Räsänen, and C. R. Proetto, Phys. Rev. B **81**, 115108 (2010).
[42] M. K. Y. Chan and G. Ceder, Phys. Rev. Lett. **105**, 196403 (2010).